doi: 10.15407/ujpe63.01.0011

E.A. NAGY, V.F. GEDEON, S.V. GEDEON, V.YU. LAZUR

Uzhgorod National University
(54, Voloshyna Str., Uzhgorod 88000, Ukraine; e-mail: viktor.gedeon@uzhnu.edu.ua)

ELECTRON-IMPACT EXCITATION OF $5^1S - 5^1P^o$ RESONANCE TRANSITION IN Sr ATOM

Main aspects of a new version of the B-spline R-matrix (BSR) method, in which nonorthogonal orbitals are applied, have been described. The BSR approximation is used to calculate the resonance structure of integral cross-sections of the $5^1S \to 5^1P^o$ transition at the electron scattering by a strontium atom in the energy interval up to 10 eV. The multiconfiguration Hartree–Fock method with a nonorthogonal set of orbitals is employed to accurately represent the target wave functions. The close-coupling expansion included 31 bound states of a neutral strontium atom ranging from the ground state to the 5s5f $^1F^o$ one. The calculated cross-sections are in good agreement with available experimental data and can be exhaustively interpreted. The structure of a resonance feature in the e-Sr scattering cross-sections at about 4 eV is discussed.

Keywords: strontium atom, electron-atom collisions, resonance transition, B-spline R-matrix method, scattering cross-sections, resonances.

1. Introduction

Practical needs stemming from the development of new types of lasers operating on electron transitions in atoms, the purposeful search for the plasma diagnostic means in devices of controlled thermonuclear fusion, the development of plasma-chemical technologies, and so forth require new methods for the calculation of atomic structures and the parameters of the electron scattering by complex atoms. In our works [1–8], we implemented the B-spline R-matrix (BSR) version of the R-matrix method. It is based on the application of nonorthogonal orbitals and B-splines as the basis functions. At present, this is one of the most efficient tools for studying the atomic structure effects in the processes of low-energy electron scattering by multielectron atoms.

In the last decade, on the basis of the proposed version of the R-matrix method, our research group regularly calculated the parameters of elementary processes, such as the elastic scattering, excitation, and ionization, which take place at collisions of slow electrons with Ca [1, 2], Mg [3], Sr [4], Si [5], F [6], Al [7], and B [8] atoms. For all indicated atomic systems, the calculation results were in good agreement with available experimental data. By such parameters as the accuracy and details of calculations, their convergence, the completeness of the account for the exchange, correlation, and resonance effects, the BSR method [1–9] has significant advantages in comparison with standard methods used in the theory of electron-atom collisions [10]. This method is especially convenient for the calculation of the electron scattering by complex atoms, when multiconfigurational wave functions of the target have to be used. All this allows us to systematically obtain correct results in the region of small and intermediate collision energies.

This work logically continues our researches of the e-Sr scattering processes, which were begun in work [4]. At present, the processes of interaction between slow electrons and strontium atoms, unlike the atoms

of other alkaline-earth elements (Mg, Ca, and Ba), remain poorly studied both experimentally and theoretically. Such situation is a strange example of the theory's pasiveness in the condition of experimental data lack, which does not of principal character, but rather is related to the difficulties in the formation of monochromatic electron and atomic beams.

At low energies, the processes of electron scattering by strontium atoms were studied for the first time in works [11, 12] using optical methods. The cited authors obtained experimental data concerning the excitation cross-sections for a large set of spectral lines of a Sr atom and their energy dependences in a rather wide interval of collision energies. Weak structural features were observed in some curves. Later, Chen *et al.* [13] measured the excitation functions (EFs) for the atomic and ionic resonance lines, as well as the energy dependences of their polarization degree. A characteristic feature was found in the EFs of the singlet $5^1S_0 \to 5^1P_1^o$ transition in a vicinity of 4 eV, which correlates by energy with the specific feature in the energy dependence of their polarization degree. The mentioned structure in the EF of the resonance line at 4 eV was explained in work [13] by cascade transitions from the 6^1S_0 level (excitation threshold of 3.79 eV) and engaging additional excitation channels.

In work [14] of the Uzhgorod experimental group headed by Prof. O.B. Shpenik, the structure of the energy spectra of electrons scattered by strontium atoms was studied using the electron spectroscopy method. In particular, the resonance features associated with the formation of short-lived negative Sr^- ions were revealed in the energy dependence of the current created by electrons elastically scattered at an angle of 90°. In the cited work [14], the resonance structure of the EF of the spectral line $\lambda = 460.7$ nm corresponding to the $5^1S_0 \to 5^1P_1^o$ transition was also discussed, and, as in work [13], a pronounced feature in the EF of the indicated resonance transition was found in a vicinity of 4 eV. According to work [14], this feature is associated not only with cascades from the upper 6^1S_0 level, but also with resonances resulting from the formation of autodetachment states of the negative Sr^- ion. Their parents are the groups of higher arranged levels, including the 6^1S_0, 6^3P_{012}, and 6^1P_1 ones. According to the estimation made by the authors of work [14], the deviation from a uniform growth of the EF of the resonance transition manifests itself already at an energy of 3.66 ± 0.05 eV, which almost coincides with the excitation threshold of the 6^3S_1 level (3.60 eV). It is evident that in order to clarify the nature of the feature in a vicinity of 4 eV in the EF of the $5^1S_0 \to 5^1P_1^o$ transition, a more detailed theoretical analysis of the structural features in the cross-sections of elementary excitations that accompany the scattering of low-energy electrons by a strontium atom is required.

In this work, the BSR method (see Section 2 and works [1–9]) was used to calculate the integral cross-sections for the electron excitation of the resonance $5^1S \to 5^1P^o$ transition in a Sr atom in the energy interval up to 10 eV. The wave functions of the Sr atomic states were calculated in the framework of the multiconfiguration Hartree–Fock (MCHF) method [15, 16]. In so doing, we considered the ground state and 30 lowest excited states of a strontium atom (BSR31 approximation) in the close-coupling expansion of the electron-atom scattering problem.

The structure of this work is as follows. The key aspects of the BSR version of the R-matrix method are expounded in Section 2.1. This version is based on the application of nonorthogonal orbitals and B-splines as the basis functions. A brief description of the electron structure in the target Sr atom is given in Section 2.2. In Section 2.3, the most important features of the computation procedure used at BSR calculations of the e-Sr collision process are summarized. Section 3 contains the results of our calculations for the integral and partial cross-sections for the electron-impact excitation of the 5^1P^o level in the Sr atom. In Section 3, we also give a physical interpretation to resonance features in the excitation cross-sections of the 5^1P^o level in a vicinity of 4 eV, which were found experimentally [13, 14].

2. Calculation Methods

2.1. General scheme of the BSR approximation

Let us briefly consider the key aspects of the BSR version of the R-matrix method, which was proposed in works [1–9]. The modification is based on the application of nonorthogonal orbitals and B-splines as the basis functions. As in the standard R-matrix method [10], the total wave function of the $(N+1)$-electron system "atom + incident electron" is taken in the form

of a series expansion,

$$\Psi_\alpha^\Gamma(X, x_{N+1}) = A\sum_{i=1}^{n}\bar{\Phi}_i^\Gamma(X;\hat{\mathbf{r}}_{N+1},\sigma_{N+1})\times$$
$$\times\frac{F_{i\alpha}^\Gamma(r_{N+1})}{r_{N+1}} + \sum_{j=1}^{m} c_j\chi_j^\Gamma(X, x_{N+1}). \quad (1)$$

Here, A is the antisymmetrization operator; $\bar{\Phi}_i^\Gamma$ the wave function of the channel formed by the vector coupling of the N-electron wave function of the target, $\Phi_i(X) \equiv \Phi_i(x_1, ..., x_N)$, with the angular, $Y_{l_T m_T}(\hat{r}_{N+1})$, and spin, $\chi_{m_S}^{1/2}(\sigma_{N+1})$, parts of the wave function of the $(N+1)$-th electron; and $x_i \equiv \equiv (\mathbf{r}_i, \sigma_i)$ stands for the set of spatial, $\mathbf{r}_i$, and spin, σ_i, coordinates of the i-th electron. In formula (1), $\chi_j^\Gamma(X, x_{N+1})$ is a set of square-integrable antisymmetrized correlation functions, which involve the effects of virtual electron capture into one of the unfilled subshells of the target and are assumed to be known together with the $\bar{\Phi}_i^\Gamma$ functions. The subscript α characterizes initial conditions and, as a result, means the input scattering channel. Our task consists in finding the radial functions for a scattered electron, $F_{i\alpha}^\Gamma$, and the expansion coefficients c_j. In the case of complex atoms, the wave functions $\Phi_i(X)$ are taken in the form of a multiconfiguration series expansion

$$\Phi_i(x_1, ..., x_N) = \sum_j c_{ij}\varphi_j(x_1, ..., x_N), \quad (2)$$

where φ_j is a given set of antisymmetrized one-configuration functions. The coefficients c_{ij} in expansion (2) can be obtained by diagonalizing the N-electron Hamiltonian of the target, H_N:

$$\langle\Phi_i|H_N|\Phi_j\rangle = E_i(Z, N)\delta_{ij}. \quad (3)$$

The basis functions φ_j and χ_j^Γ in expansions (1) and (2) are constructed from one-electron atomic orbitals φ_{α_i}. The latter, in the central-field approximation, look like

$$\varphi_{\alpha_i}(x) = \frac{1}{r}P_{n_i l_i}(r)Y_{l_i m_i}(\hat{r})\chi(m_S|\sigma), x \equiv (\mathbf{r}, \sigma), \quad (4)$$

where the notation α_i means the set of quantum numbers (n_i, l_i, m_i, m_S). In the standard Burke approach [10], in order to make calculations convenient, the radial wave functions of a scattered electron, $F_{i\alpha}^\Gamma$, are selected to be orthogonal to every atomic orbital $P_{n_j l_j}$ of the target with the same symmetry, i.e.

$$\int_0^\infty P_{n_j l_j}(r)F_{i\alpha}^\Gamma(r)dr = 0 \quad \text{at } l_j = l_i. \quad (5)$$

Evidently, this condition is purely mathematical rather than physical one and does not follow from the general quantum-mechanical principles, because the radial orbitals $P_{n_j l_j}$ and $F_{i\alpha}^\Gamma$ are eigenfunctions of different Hamiltonians.

The problem of low-energy electron scattering by an N-electron atom is reduced to a solution of the Schrödinger equation

$$(H_{N+1} - E)\,\Psi_\alpha^\Gamma(X, x_{N+1}) = 0 \quad (6)$$

with corresponding boundary conditions. Here,

$$H_{N+1} = \sum_{i=1}^{N+1}\left(-\frac{1}{2}\nabla_i^2 - \frac{Z}{r_i}\right) + \sum_{i>j=1}^{N+1}\frac{1}{r_{ij}}$$

is the Hamiltonian, and E the total energy of the $(N+1)$-electron system "atom + incident electron", and Z is the nucleus charge. The Hamiltonian H_{N+1} in Eq. (6) is diagonal with respect to the total orbital momentum L, the total spin S, their projections M_L and M_S, respectively, on the given axis, and the parity π. The function $\Psi_\alpha^\Gamma(X, x_{N+1})$, which is usually called the "collision wave function", is a completely antisymmetrized wave function of the $(N+1)$-electron system.

Substituting expansion (1) into Eq. (6), multiplying the result, in turn, by the functions $\bar{\Phi}_i^\Gamma$ and χ_j^Γ, integrating the product over all variables except for r_{N+1}, and using the orthogonality conditions for the functions $\bar{\Phi}_i^\Gamma$ and χ_j^Γ, we obtain the following system of integro-differential close-coupling (CC) equations for the functions $F_i \equiv F_{i\alpha}^\Gamma$:

$$\left(\frac{\mathrm{d}^2}{\mathrm{d}r^2} - \frac{l_i(l_i+1)}{r^2} + \frac{2Z}{r} + k_i^2\right)F_i(r) =$$
$$= 2\sum_j\left(V_{ij} + W_{ij} + X_{ij}\right)F_j(r), \quad (7)$$

where $k_i^2 = 2\,[E - E_i(Z, N)]$; and V_{ij}, W_{ij}, and X_{ij} are the local direct, nonlocal exchange, and nonlocal correlation potentials, respectively. For the electron

scattering by complex atoms, the explicit expressions for those potentials depend on the type of input data, and they are generated automatically by the BSR computation code [9].

To solve the system of CC equations (7), let us apply the BSR version of the R-matrix method, which is based on the application of nonorthogonal orbitals and B-splines as the basis functions. This approach allows various reaction types – for example, elastic scattering, electron-impact excitation and ionization of an atom – to be described within the framework of the same formalism. The main idea of the R-matrix method consists in dividing the configuration space of the system "atom + electron" into two regions: internal ($r < a$) and external ($r > a$) ones. The radius a of the internal region is selected so that the exchange and correlation effects should be rather small at $r \geq a$.

Owing to the restrictions imposed by the orthogonality conditions $\langle P_{n_j l_j} | F_i \rangle = 0$ on the collision wave function $\Psi^{\Gamma}_{\alpha}(X, x_{N+1})$, the incident electron cannot be virtually captured by one of the unfilled target subshells. The finite set of square-integrable correlation functions $\chi^{\Gamma}_j(X, x_{N+1})$ in the second sum in Eq. (1) makes it possible to partially consider the effects associated with the orthogonality conditions for the functions $P_{n_j l_j}$ and F_i, and with the confinement of the first sum in expansion (1) to a finite number of terms. However, in this case, it may result in the appearance of an unphysical pseudoresonance structure in the scattering cross-sections and can give rise to a significant increase in the number of integro-differential equations that are to be solved [10].

It is evident that, in order to take the fact that an electron can be virtually captured by an unfilled target subshells into account, it is necessary to reject the condition that the orbitals of the scattered electron F_i have to be orthogonal to the coupled target orbitals $P_{n_j l_j}$. The BSR version of the R-matrix method, which was realized in our works [1–8], advantageously differs from the modern methods of scattering theory by at least two innovations: (i) it uses nonorthogonal orbitals to represent the radial parts of the one-electron wave functions describing both the bound atomic and scattered electron states; (ii) the R-matrix basis, which is given by a complete finite set of B-splines with compact supports in the internal region, is better.

As was done in the standard R-matrix method [10], in the internal region, the total wave function of the $(N+1)$-electron system with given energy E is sought as a series expansion

$$\Psi^{\Gamma}_{E} = \sum_{k} A^{\Gamma}_{Ek} \Psi^{\Gamma}_{k} \tag{8}$$

in an energy-independent discrete basis set

$$\Psi^{\Gamma}_{k}(X, x_{N+1}) =$$
$$= A \sum_{i,j} \bar{\Phi}^{\Gamma}_{i}(X; \hat{\mathbf{r}}_{N+1}, \sigma_{N+1}) \frac{u_j(r_{N+1})}{r_{N+1}} c^{\Gamma}_{ijk} +$$
$$+ \sum_{i} \chi^{\Gamma}_{i}(X, x_{N+1}) d^{\Gamma}_{ik}, \tag{9}$$

where the functions $\bar{\Phi}^{\Gamma}_{i}$ and χ^{Γ}_{i} are defined as in formula (1). The functions $F^{\Gamma}_{i\alpha}$ describing the radial motion of the scattered electron in the i-th channel are presented in expansion (9) as linear combinations of a finite number of basis functions u_j that satisfy the boundary conditions $u_j = 0$ and $(a/u_j)du_j/dr|_{r=a} = b$, where b is an arbitrary real constant. For the basis functions of this type, Hamiltonian (6) is not Hermitian in the internal region owing to nonzero (at $r = a$) surface terms, which arise from the kinetic energy operator. However, those terms can be excluded with the help of the Bloch operator L_{N+1} [10]. Then, the formal solution (1) of the Schrödinger equation (6) reads

$$|\Psi\rangle = 1/2 \sum_{kj} |\Psi^{\Gamma}_{k}\rangle \langle \Psi^{\Gamma}_{k} | \bar{\Phi}^{\Gamma}_{j} \rangle (E_k - E)^{-1} \times$$
$$\times (d/dr_{N+1} - b_j/r_{N+1}) \langle \bar{\Phi}^{\Gamma}_{j} | \Psi \rangle. \tag{10}$$

By projecting this equation on the channel functions $\bar{\Phi}^{\Gamma}_{i}$ and performing calculations at the internal region boundary, we obtain

$$F^{\Gamma}_{i}(a) = \sum_{j=1}^{n} R^{\Gamma}_{ij}(E) \left(a \frac{dF^{\Gamma}_{j}}{dr_{N+1}} - b_j F^{\Gamma}_{j} \right)_{r_{N+1}=a}, \tag{11}$$

where the R-matrix with the elements

$$R^{\Gamma}_{ij}(E) = \frac{1}{2a} \sum_{k} \frac{w^{\Gamma}_{ik}(a) w^{\Gamma}_{jk}(a)}{E^{\Gamma}_{k} - E}, \tag{12}$$

the radial functions F^{Γ}_{i}, and the surface amplitudes w^{Γ}_{ik} were introduced. By diagonalizing the matrix

$\langle\Psi_k^\Gamma|H_{N+1} + L_{N+1}|\Psi_{k'}^\Gamma\rangle_{\rm int}$ for each set of quantum numbers Γ, we can determine the energies E_k^Γ and the coefficients c_{ijk}^Γ and d_{ik}^Γ in the series expansion (9), i.e. the wave functions Ψ_k^Γ for the corresponding basis states. However, this procudure should be fulfilled only once in order to determine the R-matrix in the whole interval of collision energies.

As was indicated above, in most cases, the inclusion of additional correlation functions χ_i^Γ into the initial series expansion (9) results in the appearance of a pseudo-resonance structure in the scattering cross-sections and additional integro-differential equations that follow from series expansion 9) and are required for realistic calculations of complex atoms.

The BSR version of the R-matrix method, which is based on the application of nonorthogonal orbitals and B-splines as the basis functions and was realized in our works [1–8], is free from those difficulties. The indicated choice of $u_j(r)$ provides a rapid convergence of the R-matrix expansion without introducing the so-called Buttle corrections (see work [10]) into the diagonal R-matrix elements (12). The basis splines have excellent properties, as if they were cially created for the R-matrix theory. They form a complete basis in the finite R-matrix interval $[0, a]$ and are convenient for the determination of the coupled target orbitals and the orbitals of a scattered electron. The convenience is provided first of all by the fact that the B-splines are finite functions that are different from zero only in their support intervals.

The next step consists in the determination of the K- and S-matrices and the phase shifts. Since $r > a$ in the external region, all exchange and correlation potentials are almost equal to zero. Therefore, rather a simple system of coupled integro-differential equations is obtained for the radial functions $F_i(r)$ in this region. They can be solved numerically with a sufficient accuracy making use of modern computers, providing unambiguous results. The obtained solutions are matched at $r = a$ with the solutions in the internal region ($r < a$). Then it is easy to determine the K-matrix from the asymptotic relation

$$F_{i\alpha} \underset{r\to\infty}{\sim} k_i^{-1/2}(\delta_{i\alpha}\sin\theta_i + K_{i\alpha}\cos\theta_i), \qquad (13)$$

where θ_i is the asymptotic phase of the regular Coulomb functions (see, e.g., work [10]), and the subscript α indicates the channel number of the incident wave. The scattering, $S_{i\alpha}$, and transition, $T_{i\alpha}$, $(n \times n)$-matrices can be determined with the help of the known matrix relation

$$\mathbf{S} = \mathbf{1} + \mathbf{T} = (\mathbf{1} + i\mathbf{K})/(\mathbf{1} - i\mathbf{K}).$$

In what follows, those matrices are used for the calculation of scattering cross-sections and all other observable quantities.

From the computational viewpoint, the most important properties of the basis splines B_i with compact support were described, e.g. , in work [9]. In the cited work, spline algorithms for the solution of integro-differential equations obtained in the framework of the scattering and bound-state problems were also considered in detail. It should be emphasized that those algorithms have two principal advantages over the algorithms based on the finite-difference approximation. First, the local properties of spline algorithms, which are provided by the finite properties of basis splines with compact support, are especially important for numerical calculations. Second, owing to the finiteness and completeness of the finite system of B-splines, the integro-differential equations, after their discretization in the internal R-matrix region ($r < a$), are reduced to a system of finite-rank matrix-vector equations with sparse matrices (namely, band ones), which significantly simplifies the numerical analysis of such systems.

In our works [1–8], general approaches to the problem of electron correlation and its account were also described. In particular, this is the B-spline MCHF method. It is based on the representation of the radial orbitals $P_{nl}(r)$ as finite expansions in the complete basis set of B-splines $\{B_i\}_{i=1}^{n_S}$. A multiconfiguration character of the series expansion for the total wave function $\Phi_i(X)$ of the N-electron system (2) allows one to make allowance for a considerable number of correlation effects.

A quantum-mechanical calculation in the framework of the MCHF method consists of two stages. These are the creation of a multielectron basis for the configuration state functions (CSFs) and the solution of multiconfiguration Hartree–Fock equations, from which the radial wave functions $P_{nl}(r)$ entering the Slater determinants are determined. Success in any practical calculation of atomic characteristics strongly depends on the choice of radial orbitals $P_{nl}(r)$ and configurations that are included in the series expansion of the target wave function in the CSF

basis. Unlike the standard approach [10], the applied version of the R-matrix method uses nonorthogonal coupled orbitals as one-electron functions. They are optimized in independent MCHF calculations for every term. The application of those orbitals is crucial for the adequate description of a complicated resonance structure in the scattering cross-sections of an electron by multielectron atoms.

2.2. Electron structure calculation for a Sr atom

Let us now consider the specific features in the application of the B-spline MCHF method to calculate the energy structure of a Sr atom. Various approximations of this method differ from one another by the number and choice of basis configurations that are taken into account in the series expansion of the traget states and pseudo-states $\Phi_i(X) \equiv \equiv \Phi_i(x_1, ..., x_N)$. In our calculations, the relevant expansion included the ground state and 30 lowest excited spectroscopic states of a Sr atom, up to the $5s5f\ {}^1F^o$ state inclusive. All those states are energetically allowed (i.e. they correspond to the so-called open channels) at the collision energies concerned. The wave functions of coupled atomic states obtained at that are used to determine the parameters of the e-Sr scattering, so that they should contain rather compact configuration expansions.

Strontium, together with its ground state configuration $[1s^2 2s^2 2p^6 3s^2 3p^6 3d^{10} 4s^2 4p^6] 5s^2\ {}^1S$ and singly excited states $4p^6 5snl\ {}^{3,1}L$, is similar in many respects to helium. In other words, under certain conditions, it can be considered in the framework of the model of two electrons above a Kr-like $[1s^2 2s^2 2p^6 3s^2 3p^6 3d^{10} 4s^2 4p^6]$-core obtained by the double ionization of a Sr atom. To simplify notations, the closed shells of a Sr^{2+} ion will be omitted in the further consideration. For the ground state and for lower excited states of Sr, both the valence and core-valence correlations are important. Bearing all that in mind, we included the electron configurations with the excited core into the MCHF expansion of the target wave function.

The calculation procedure for the target states includes the following steps. It begins from the generation of the Sr^{2+} core orbitals in the Hartree–Fock approximation. As a result of calculations with the "frozen" core, we obtain the valence $5s$, $5p$, and $4d$ orbitals for Sr^+. The application of the most coupled channels in the MCHF expansion makes it possible to take a considerable part of the valence correlation into account. At the same time, the core-valence correlation is made allowance for by including the additional electron configurations $p^5 \overline{n}l\overline{n}'l'$ into the MCHF expansion:

$$\phi(4p^6 nl) = a_{nl}\phi_{\rm HF}(4p^6 nl) + \\ + \sum_{\bar{n}l\bar{n}'l'} b_{\bar{n}l\bar{n}'l'}\chi(4p^5 \bar{n}l\bar{n}'l'), \qquad (14)$$

where the bar over the symbols marks the correlation orbitals rather than the physical ones. In other words, the Hartree–Fock wave functions $\phi_{\rm HF}\left(4p^6 nl\right)$ are appended here by the correlation functions χ with a $4p$-excited core.

The described structural calculations were carried out making use of the MCHF software [15, 16]. Since the average radius of nl orbitals lies between the average core radius and the radii of valence orbitals, this method allows the core-valence correlation to be effectively taken into account with the help of rather a small number of electron configurations. Note also that the correlation nl orbitals were optimized in independent calculations for each state separately. When generating the lower states of a Sr atom using the MCHF method, the core-valence states of Sr^+ ion were used as initial ones.

The corresponding multichannel series expansion of the target atom states has the following structure:

$$\Phi(4p^6 5snl, LS) = \mathcal{A}\sum_{nl}\left\{\phi(4p^6 5s)P(nl)\right\}^{LS} + \\ + \mathcal{A}\sum_{nl}\left\{\phi(4p^6 5p)P(nl)\right\}^{LS} + \\ + \mathcal{A}\sum_{nl}\left\{\phi(4p^6 4d)P(nl)\right\}^{LS}, \qquad (15)$$

where $\mathcal{A}$ is the antisymmetrization operator. To simplify notations, we assume that the expansion coefficients in formula (15) are included into the unknown radial functions $P(nl)$ for the external valence electron. Those functions were expanded in the B-spline basis, and the corresponding equations were solved provided that the wave functions vanish at the boundary of the internal R-matrix region. The described scheme gives a set of orthogonal one-electron orbitals for each bound state. However, orbitals from different sets are not orthogonal to one another. This procedure is often mentioned in the literature as the application of "nonorthogonal orbitals" and will be used

below in this sense. Finally, we use the same multichannel series expansion (14) for both the $5snl$ states and all nl^2 states with equivalent electrons. The number of physical states that can be generated in this method depends on the size a of the R-matrix box. By choosing $a = 80a_0$, where $a_0 = 0.529 \times 10^{-10}$ m is the Bohr radius, we obtain the adequate description of all lower Sr states up to the $5s5f\ ^1F^o$ one.

In this work, we included 119 B-splines of the eighth order into the calculations. Since the abovementioned calculations of coupled atomic states using the B-spline MCHF method generate different sets of nonorthogonal orbitals, their further usage becomes some complicated. On the other hand, our configuration series expansions for the atomic states of Sr target contain from 50 to 270 configurations, so that they can be used to calculate collisions, by using rather modest computational resources.

In Table 1, the results of calculations of the excitation energies for 31 spectroscopic states of a Sr atom are compared with experimental data [18]. In general, the agreement between the experimental and theoretical results is rather good, with the energy deviations not exceeding 0.1–0.2 eV (and somewhere 0.01 eV). The only exception is the $4d5p\ ^1F^o$ state, for which the effects of electron correlations have to be taken into account more carefully. The calculation accuracy obtained for the structure of a Sr atom (the energies of levels, the wave functions) was significantly higher in comparison with the accuracy of results used in our previous theoretical researches of the e-Sr scattering (see, e.g., works [19–23]). Note also that analogous calculations of the Ca [1] and Mg [3] coupled atomic states were performed not in the MCHF approximation [15, 16], but in the framework of the close-coupling method with basis splines localized in the R-matrix box [17]. However, in the case of Sr atom (the nucleus charge $z = 38$), such calculations, as well as the account for the spin-orbit interaction, go beyond our actual computational capabilities.

2.3. e-Sr collision calculations

Calculations of the processes of electron scattering by a Sr atom were carried out in the B-spline R-matrix approximation (the BSR soft code [9]). The problem of e-Sr scattering in the internal R-matrix region ($r \le a$) was solved similarly to Eq. (9) by expanding the collision wave function in the discrete basis,

$$\Psi_k^\Gamma(x_1, ..., x_{N+1}) =$$
$$= A \sum_{i,j} \bar{\Phi}_i^\Gamma(x_1, ..., x_N; \hat{\mathbf{r}}_{N+1}, \sigma_{N+1}) \times$$
$$\times r_{N+1}^{-1} B_j(r_{N+1}) c_{ijk}^\Gamma, \qquad (16)$$

where $\bar{\Phi}_i^\Gamma$ are the wave functions of the channels. Here, we expanded the radial wave functions of the continuum, $F_{i\alpha}^\Gamma$, in the finite system of basis splines

Table 1. **Excitation energies (in eV) for 31 lower spectroscopic states of the Sr target. Theoretical E_{theor} values are compared with Moore's experimental data [18]. Triplet energies are averaged over the term. $\Delta E = E_{\text{exp}} - E_{\text{theor}}$**

No.	State	E_{exp} [18]	E_{theor}	ΔE
1	$5s^2\ ^1S$	0.0	0.0	0.0
2	$5s5p\ ^3P^o$	1.823	1.847	−0.024
3	$5s4d\ ^3D$	2.264	2.272	−0.008
4	$5s4d\ ^1D$	2.499	2.480	0.019
5	$5s5p\ ^1P^o$	2.691	2.673	0.018
6	$5s6s\ ^3S$	3.601	3.633	−0.032
7	$5s6s\ ^1S$	3.793	3.714	0.079
8	$4d5p\ ^3F^o$	4.173	4.111	0.062
9	$4d5p\ ^1D^o$	4.195	4.196	−0.001
10	$5s6p\ ^3P^o$	4.207	4.222	−0.015
11	$5s6p\ ^1P^o$	4.228	4.241	−0.013
12	$5s5d\ ^1D$	4.306	4.311	−0.005
13	$5s5d\ ^3D$	4.344	4.361	−0.017
14	$5p^2\ ^3P$	4.406	4.408	−0.002
15	$4d5p\ ^3D^o$	4.519	4.568	−0.049
16	$5p^2\ ^1D$	4.583	4.499	0.084
17	$5p^2\ ^1S$	4.608	4.590	0.018
18	$4d5p\ ^3P^o$	4.628	4.767	−0.139
19	$5s7s\ ^3S$	4.641	4.579	0.062
20	$4d5p\ ^1F^o$	4.713	4.944	−0.231
21	$5s7s\ ^1S$	4.767	4.954	−0.187
22	$5s4f\ ^3F^o$	4.805	4.734	0.071
23	$5s7p\ ^1P^o$	4.825	4.810	0.015
24	$5s7p\ ^3P^o$	4.891	4.885	0.006
25	$5s4f\ ^1F^o$	4.903	4.754	0.149
26	$5s6d\ ^3D$	4.922	4.885	0.037
27	$5s6d\ ^1D$	4.927	4.859	0.068
28	$5s8s\ ^3S$	5.054	5.008	0.046
29	$5s8s\ ^1S$	5.091	5.216	−0.125
30	$5s5f\ ^3F^o$	5.129	5.049	0.080
31	$5s5f\ ^1F^o$	5.148	5.140	0.008

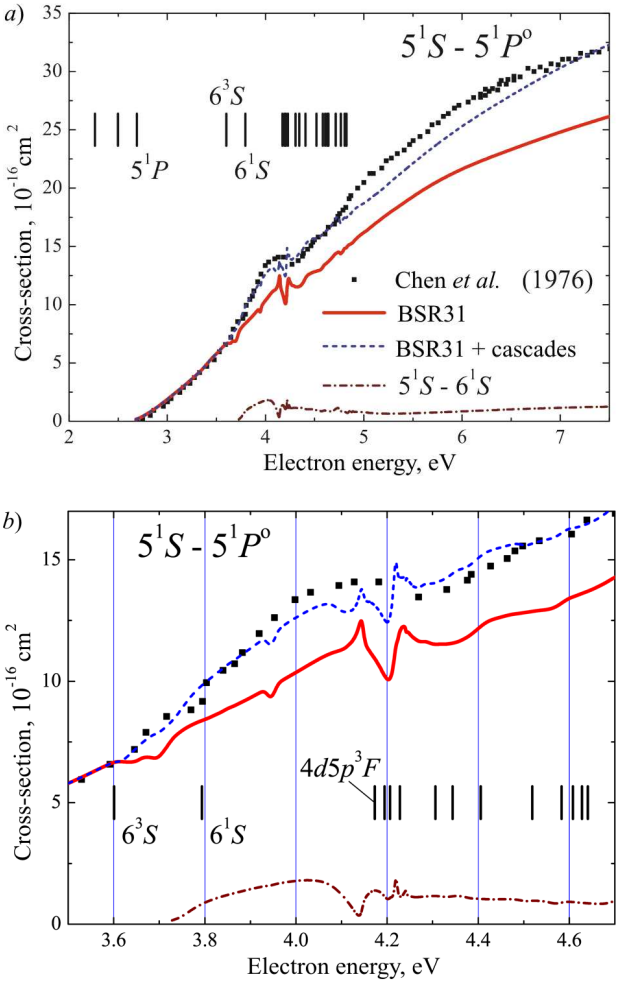

Fig. 1. Energy dependences of the ICS for the $5^1S \to 5^1P^o$ transition at the e-Sr scattering. The results of BSR31 calculation (taking and not taking the cascade contribution into account) are compared with the experiment by Chen *et al.* [13]. The ICS for the $5^1S \to 6^1S$ transition and the experimental excitation thresholds for the lower Sr levels [18] are shown (a). The scaled-up fragment of panel a in a vicinity of 4 eV (b)

$B_j(r)$ given in the R-matrix interval $0 \le r \le a$. The amplitudes of wave functions at the $r = a$ boundary, which are required to evaluate the R-matrix, are determined by the coefficient in front of the last B-spline; just this spline is the only basis spline that differs from zero at the internal region boundary. The number of B-splines and the R-matrix radius in the scattering calculations were taken the same as when calculating the coupled target states. The partial wave contributions were calculated numerically

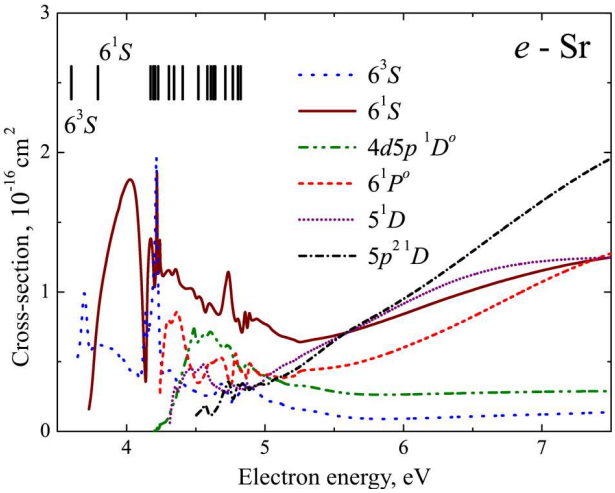

Fig. 2. Energy dependences of ICSs for the excitation of 6^3S, 6^1S, $4d5p\ ^1D^o$, 6^1P^o, 5^1D, and $5p^2\ ^1D$ from the ground level 5^1S at the e-Sr scattering obtained in the BSR31 approximation. The excitation thresholds of the lower Sr levels [18] are indicated

up to $L = 50$. When evaluating the contributions from higher L-values, the procedure of "remnant summation" was used as appropriate, which is based on an approximation by geometrical series [9]. The cross-sections were calculated, by following the standard R-matrix procedure with the use of the FARM soft package [24] for the external region.

In order to simplify the calculations of the e-Sr scattering and take the resonance structure into account most consistently, the experimental excitation energies of the target [18] were not applied. Instead, we used their values calculated with the help of the MCHF soft code [15, 16] and using B-splines (see Table 1).

3. Results and Their Discussion

Let us compare the integral cross-sections (ICSs) calculated for the resonance transition excitation of a Sr atom with the experimental data by Chen *et al.* [13]. In Fig. 1, the ICSs for the $5^1S \to 5^1P^o$ transition at the e-Sr scattering are shown. Together with the experimental EFs [13], the ICSs calculated in the BSR31 approximation taking and not taking into account cascades from higher levels are also depicted.

In order to estimate the maximum possible contribution of cascades, Fig. 2 demonstrates the energy dependences of EFs for the electron-impact excitation

of several higher states (6^3S, 6^1S, $4d5p\ ^1D^o$, 6^1P^o, 5^1D, and $5p^2\ ^1D$) of a Sr atom. At collosion energies in a vicinity of 4 eV, which are of interest for the comparison with the experiment, the radiative decay of those states to the 5^1P^o level expectedly results in an appreciable cascade contribution to the EF, which can be experimentally observed [13].

On the other hand, a comparison of the ICSs exhibited in Figs. 1 to 3 testifies that, in the energy interval from 3.6 to 4.2 eV, the mentioned cascade contribution to the $5^1S \to 5^1P^o$ transition cross-section can be made only by transitions from the higher excited states, the 6^3S and 6^1S ones, with a considerably prevailing contribution of the $6^1S \to 5^1P^o$ transition. Figures 1 and 2 illustrate an almost complete agreement between the theoretical (the BSR31 approximation taking cascades into account) and experimental [13] results in the energy interval from 2.69 eV (the excitation threshold) to 4.8 eV, as well as above 6.8 eV. A convex structure at about 4 eV in the energy dependence of the ICS for the $5^1S \to 5^1P^o$ transition is a result of both the resonance features in the ICS of the direct excitation of the 5^1P^o level and the radiative decay of the higher excited state 6^1S.

In Fig. 3, the BSR31 cross-sections calculated for the direct $5^1S \to 5^1P^o$ transition in a Sr atom are compared with experimental data [14]. Besides the initial EFs [14], the same dependences, but calibrated by shifting them by 0.21 eV to the right and multiplied by 1.2, are also plotted. Figure 3 demonstrates remarkable agreement between the fitted experimental EF [14] with our calculated ICS of the resonance transition in the energy interval from the excitation threshold to 4.8 eV.

In order to analyze the resonance structure of the excitation ICS for the dipole $5^1S \to 5^1P^o$ transition, the expansion of this cross-section in the partial waves $^2P^o$, ^2D, and ^2G is shown in Fig. 4. A similar expansion of the excitation ICS for the $5^1S \to 6^1S$ transition is exhibited in Fig. 5. The contributions made by two other partial waves, ^2S and $^2F^o$, to the resonance structure of the ICSs of the mentioned transitions are insignificant and therefore are not depicted in Figs. 4 and 5.

From Fig. 4, it is evident that the convex resonance structure at about 3.6–4.3 eV in the theoretical ICSs for the $5^1S \to 5^1P^o$ transition is substantially governed by the behavior of the partial ^2G wave. In Fig. 6, the partial ^2G cross-sections for the excitation from the ground 5^1S state of a Sr atom to the states 4^3D, 4^1D, 5^1P^o, and 6^1S are exhibited. As one can see from Figs. 4 and 6, the dominating resonance structure in the partial cross-sections of the 5^1P^o and 4^3D excitations for the ^2G wave looks like

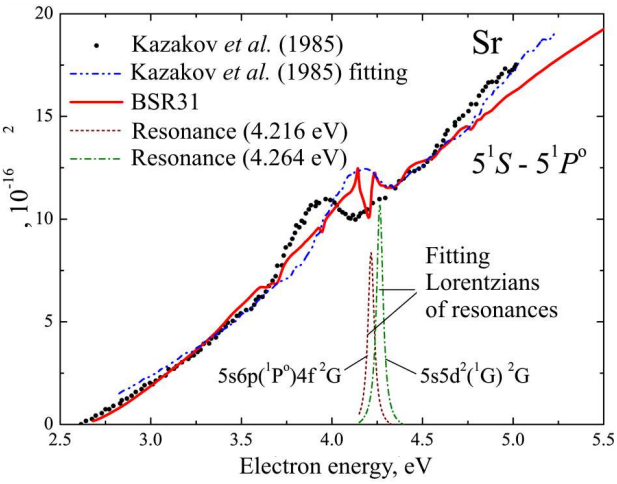

Fig. 3. Energy dependences of the ICS for the $5^1S \to 5^1P^o$ transition at the e-Sr scattering. The results of BSR31 calculations are compared with the experiment by Kazakov *et al.* [14]. The experimental EFs are shown together with the same functions, but calibrated by shifting them by 0.21 eV to the right and multiplying by 1.2. The fitting Lorentzians for the $5^1S \to 6^1S$ transition are also shown and the experimental excitation thresholds for the $5s6p(^1P^o)4f\ ^2G$ (at 4.216 eV) and $5s5d^2(^1G)\ ^2G$ (at 4.264 eV) resonances are indicated

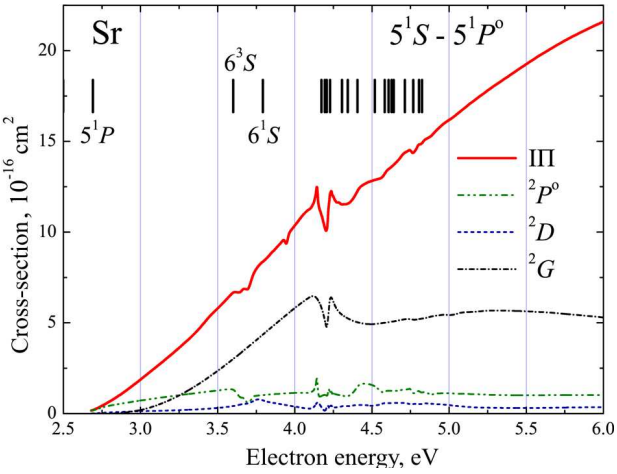

Fig. 4. Energy dependences of the integral and partial $^2P^o$, ^2D, and ^2G cross-sections for the $5^1S \to 6^1S$ transition at the e-Sr collision (the BSR31 approximation). The excitation thresholds for the lower Sr levels [18] are indicated

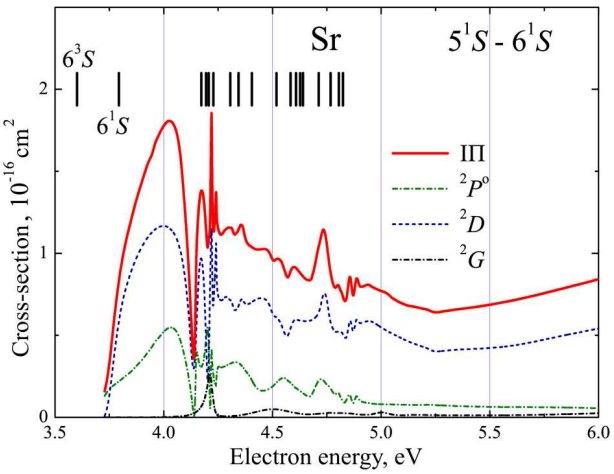

Fig. 5. Energy dependences of the integral and partial $^2P^o$, ^2D, and ^2G cross-sections for the $5^1S \to 5^1P^o$ transition at the e-Sr collision (the BSR31 approximation). The excitation thresholds for the lower Sr levels [18] are indicated

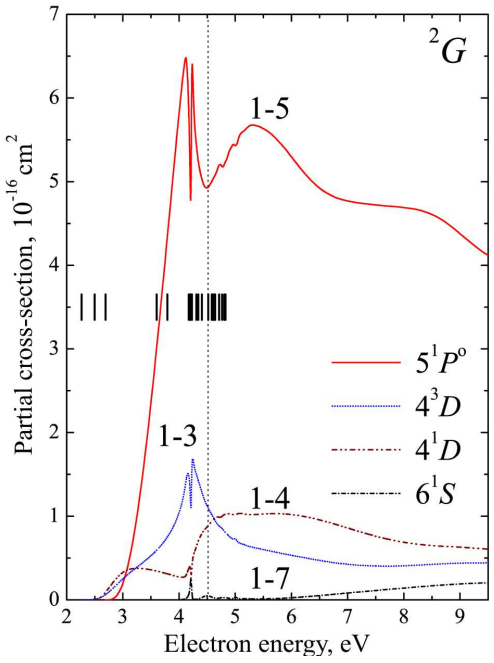

Fig. 6. Energy dependences of the ^2G partial cross-sections for the transitions from the ground state 5^1S to the states 5^1P^o, 4^3D, 4^1D, and 6^1S at the e-Sr collision (the BSR31 approximation). The excitation thresholds for the lower Sr levels [18] are indicated. The vertical dotted line is drawn to facilitate a comparison of resonance structures in the cross-sections of different transitions. The numbers of states in the notations of transitions from the initial state to the final one are indicated in accordance with Table 1

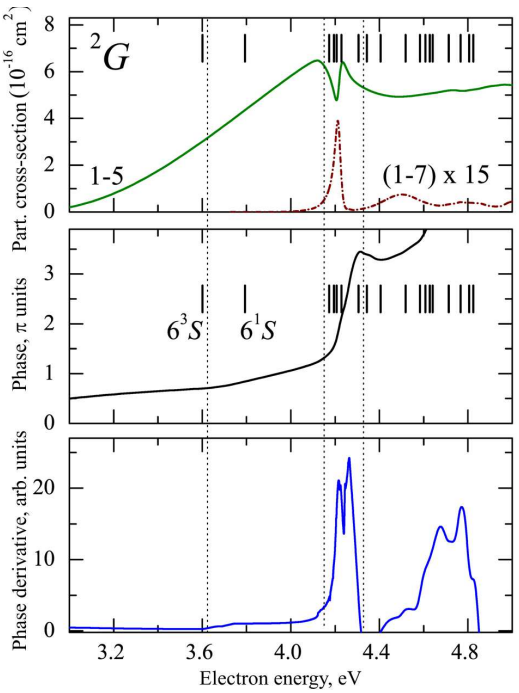

Fig. 7. Example of the partial-phase analysis used for the detection and classification of resonance features in the ^2G wave. Cross-sections and phases were obtained in the BSR31 approximation. Vertical dotted lines are drawn to facilitate a comparison of resonance structures in different panels. The numbers of states in the notations of transitions from the initial state to the final one are indicated in accordance with Table 1

a wide peak in a vicinity of about 4 eV. A bifurcation of the mentioned convex structure in an energy interval of 4.1–4.2 eV is also observed. This phenomenon is a result of imposing two narrow resonances of the Feshbach type on the shape resonance (see Fig. 3).

A somewhat different scenario takes place for the ICS of the $5^1S \to 6^1S$ transition (see Fig. 5). Here, the ICS behavior is governed by the character of the energy dependences of the partial cross-sections for the ^2D and, to some extent, $^2P^o$ waves.

In order to detect and classify the resonance structure in the integral cross-sections of the e-Sr scattering, we carried out their partial-wave analysis, which was based on the calculation of the sum of characteristic phases for each partial wave. Illustrative examples of this kind for the ^2G, ^2D, and $^2P^o$ waves are shown in Figs. 7, 8, and 9, respectively. The energy regions, where the sum of characteristic phases δ increases by π, were recalculated with a small energy step down to 10^{-4} eV. It was done in order to determine the deriva-

tive of the sum of characteristic phases with respect to the energy with a higher accuracy. In the resonance region, this derivative looks like a Lorentzian, whose maximum determines the resonance position, and the resonance width equals $2/(d\delta/dE)$.

Unfortunately, the R-matrix method gives no direct "recipe" for the detection and classification of resonances in the ICS of the scattering in the given energy interval. It also does not point to a spectroscopic "identity" (affiliation) of the transient quasistationary state of the negative ion that is responsible for a resonance feature in the ICS of the scattering. Thus, the identification of a resonance and the determination of its parameters requires considerable additional efforts.

Table 2 contains the parameters of the resonances that were revealed in a vicinity of 4 eV, when analyzing the results of BSR31 calculations. Figures 7 to 9 illustrate the main stages of this analysis for the above-mentioned partial waves ^2G, ^2D, and $^2P^o$. Each of the figures includes three panels. The upper panel demonstrates the fragments of the energy dependences of partial cross-sections for the $5^1S \rightarrow 5^1P^o$ and $5^1S \rightarrow 6^1S$ transitions. The energy dependence of the sum of characteristic phases for the relevant partial wave (in π-units) is shown in the middle panel, and the energy derivative of this dependence is exhibited in the lower panel.

It should be recalled that a certain resonance structure in the energy dependence of the partial cross-section is interpreted as a "true" resonance, if two accompanying factors are available: (i) the phase has a jump of about π in the energy interval, where the feature in the partial cross-section manifests itself, and

Table 2. **Resonance parameters for the *e*-Sr collisions in a vicinity of 4 eV**

No.	Configuration	Term	Energy, eV	Width, meV
1	$5s6s(^3S)5d$	^2D	3.719	162
2	$5s5p(^1P)4f$	^2G	4.087	559
3	$4d^2(^1D)5p$	$^2P^o$	4.146	17
4	$4d5p^2(^1D)$	^2D	4.147	50
5	$5s6p^2(^1D)$	^2D	4.207	27
6	$5s6p(^1P^o)4f$	^2G	4.216	33
7	$5s6p(^1P^o)5d$	$^2P^o$	4.216	16
8	$5s6p(^1P^o)4f$	^2D	4.222	3.4
9	$5s5d^2(^1D)$	^2D	4.242	1.3
10	$5s5d^2(^1G)$	^2G	4.263	46

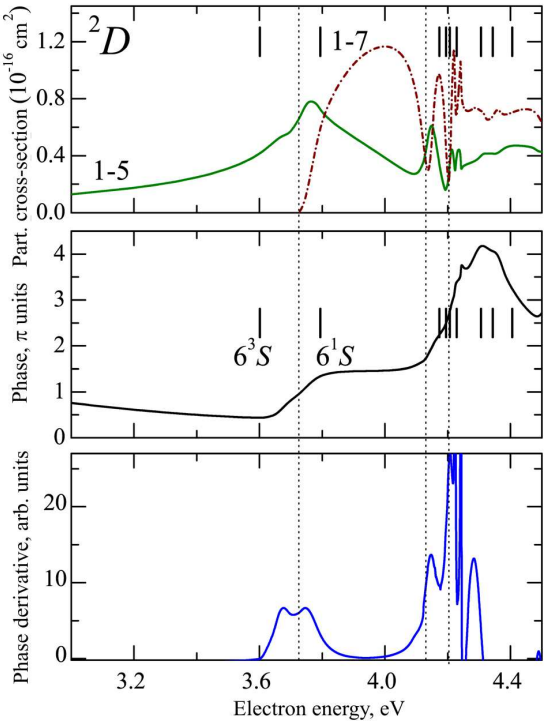

Fig. 8. The same as in Fig. 7, but for ^2D wave

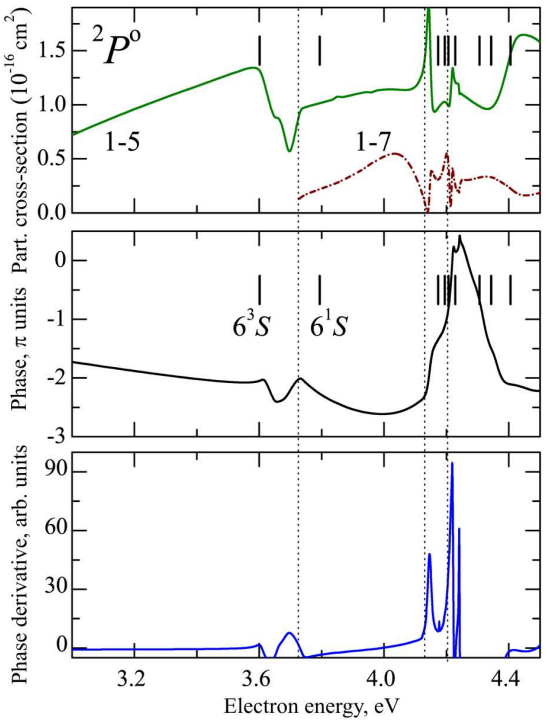

Fig. 9. The same as in Fig. 7, but for $^2P^o$ wave

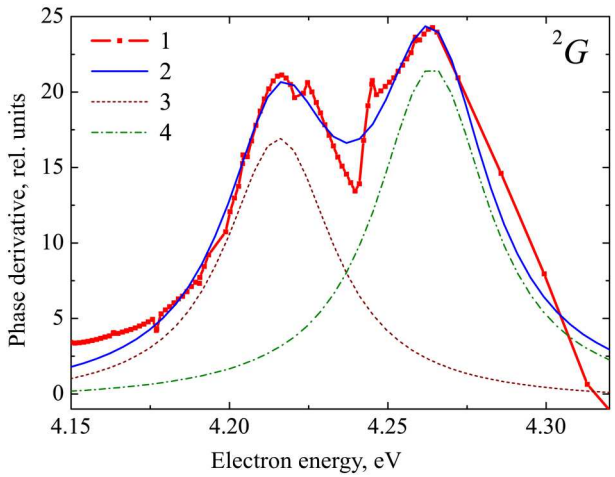

Fig. 10. Lorentzian fitting of the energy derivative of the phase sum for the ^2G partial wave in an energy interval of 4.15–4.32 eV: the derivative of the phase sum calculated in the BSR31 approximation (*1*); the resulting fitting curve (*2*); fitting Lorentzians for resonances with peaks at energies of 4.216 and 4.264 eV, respectively (*3, 4*) (Table 2)

(ii) the derivative of the phase has a Lorentzian shape at the indicated energies. As was marked above, the position of the Lorentzian maximum on the energy scale is considered to be the energy of the resonance with the width $2/(d\delta/dE)$. This "perfect" picture can be violated (i) if new scattering channels become open, i.e. near the excitation thresholds for the target-atom states and (ii) if the scattering cross-sections include wide-shape resonances, for which the phase jump rearly reaches a value of about π.

In particular, in Fig. 7, the energy dependence of the phase sum for the partial ^2G wave in the near-threshold energy region is depicted. Its behavior has a typical character (see, e.g., works [1, 6]), when a wide shape resonance (in our case, $5s5p(^1P^o)4f\ ^2G$) is suppressed by the opening of new collision channels at 4.17–4.22 eV. The ^2G phase starts to grow above 3.6 eV and increases by almost 0.7π. The phase analysis in this energy region also revealed a two-peak structure in the energy derivative of the phase sum for the ^2G wave. This structure can be approximated rather accurately by a pair of Lorentzians (Fig. 10). It should be emphasized that the powerful $5s5p(^1P^o)4f\ ^2G$ resonance at 4.087 eV is located above the "parent" $5s5p(^1P^o)$ state, and it can be considered as a shape resonance. At the same time, two other states, $5s6p(^1P^o)4f\ ^2G$ (at 4.216 eV) and $5s5d^2\ (^1G)\ ^2G$ (at 4.264 eV), lie below the excitation thresholds of their "parent" states $5s6p(^1P^o)$ and $5s5d(^1D)$, respectively, and are classified as Feshbach resonances.

Hence, our researches of the resonance structure in the excitation ICS of the $5^1S \to 5^1P^o$ transition in a vicinity of 4 eV confirm, in general, the conclusions made in the work by Kazakov *et al.* [14] that the levels located above the threshold of the 6^3S state are excited through the formation of a short-lived negative Sr^- ion. The authors of work [14] assumed that, besides cascade transitions, a contribution to the structure observed near 4 eV can be given by a state of the negative Sr^- ion with the configuration $5s5p6s$ ($E_0 = 3.92 \pm 0.03$ eV). However, as was shown above, it is the above-threshold shape resonance in the ^2G wave that is "responsible" for the discussed structure. This resonance cannot appear due to the contribution made by the $5s5p6s$ configuration states. Most likely, it is a result of the formation of a quasistationary state of the Sr^- ion with the $5s5p\ (^1P^o)4f$ configuration.

Cascade transitions from the 6^1S level are another important factor that affects the formation of the convex peculiarity in the energy dependence of the ICS for the 5^1P^o excitation in the energy interval 3.8–4.2 eV. From Fig. 5, one can see that (i) the contribution of the partial ^2D wave prevails in the integral excitation cross-section of the $5^1S \to 6^1S$ transition and completely determines its shape at the indicated energies, and (ii) the convex structure observed in the energy dependence of the ^2D partial cross-section has a typical form of shape resonance (see, e.g., work [25]), which is associated with the formation of the quasistationary $5s6s(^1S)5d\ ^2D$ state of the negative Sr^- ion. However, the absence of a jump in the ^2D phase at energies of 3.8–4.2 eV (Fig. 8) does not allow this feature to be considered as a "true" resonance. In our opinion, such a phase behavior is a combined result of several factors: (i) a rather considerable inaccuracy at the determination of the relative arrangement of energy levels for the 6^3S and 6^1S states, which reaches 0.12 eV in the case concerned; (ii) a high correlation degree of the resonance processes that are sensitive to the slightest computational mismatches; and (iii) the presence of the ^2D-shape resonance $[5s6s(^3S)5d\ ^2D]$ 162 meV in widthat an energy of 3.719 eV, which occurs at the excitation threshold of the obscured $5s6s(^1S)5d\ ^2D$ shape resonance. In this case, the con-

clusion suggests itself that a detailed calculation for the target structure is required with the application of the BSR soft package [9].

4. Conclusions

The energy dependence of the experimental excitation cross-section of the $5^1S \to 5^1P^o$ transition in a Sr atom by the electron impact [13, 14] includes a pronounced structure in an energy interval at about 4 eV. Till now, this structure has not obtained an adequate theoretical interpretation. Since deviations from the smooth behavior of the integral excitation cross-section [13] of the 5^1P^o level begins at about 3.79 eV, we supposed that this peculiarity is a result of the cascade-transition contribution from the 6^1S level and the opening of new excitation channels (see Fig. 1). However, deviations from the monotonic growth of the excitation function experimentally manifested itself already at an energy of about 3.66 eV [14], which is close to the excitation potential of the 6^3S level (3.59 eV). The authors of work [14] also asserted that the pronounce structure in the ICS is a result of the contributions made not only by cascade transitions, but also by the states of the negative Sr^- ion with the $5s5p6s$ configuration (at about 3.92 eV).

In this work, the ICS for the electron-impact excitation of the 5^1P^o level of a Sr atom has been studied in the subthreshold energy interval, by using the BSR31 approximation. It is shown the following. (i) A convex feature in a vicinity of about 4 eV in the experimental EFs for the $5^1S - 5^1P^o$ transition [13, 14] is associated, first of all, with the contribution of ^2G resonances in the cross-section of the direct 5^1P^o excitation, as well as the cascade contribution from the 6^1S level. (ii) The main contribution to the discussed ICS structure of the direct 5^1P^o excitation in a vicinity of 4 eV is made by the shape resonance $5s5p(^1P^o)4f\ ^2G$ with a maximum at about 4.1 eV with two imposed narrow Feshbach resonances $5s6p(^1P^o)4f\ ^2G$ and $5s5d^2(^1G)\ ^2G$ (at 4.216 and 4.264 eV, respectively). (iii) The dominating contribution to the excitation ICS of the 6^1S level is given by the obscured $5s6s(^1S)5d\ ^2D$ shape resonance, which turns out destroyed by a few accompanying resonance formations in the same ^2D partial wave. In other words, the convex feature in a vicinity of 4 eV, which was revealed in the energy dependences of the cross-sections of a Sr-atom 5^1P^o excitation by the electron impact [13, 14], has a resonance origin and is governed, to a large extent, by highly correlated processes of the formation and decay of quasistationary states of the negative Sr^- ion, which are difficult to be described theoretically.

The authors express their gratitude to Prof. A. Zatsarinny and Prof. K. Bartschat (Drake University, Des Moines, Iowa, USA) for their help in carrying out calculations and fruitful discussion.

1. O. Zatsarinny, K. Bartschat, S. Gedeon, V. Gedeon, V. Lazur. Low-energy electron scattering from Ca atoms and photodetachment of Ca^-. *Phys. Rev. A* **74**, 052708 (2006).
2. O. Zatsarinny, K. Bartschat, L. Bandurina, S. Gedeon. Electron-impact excitation of calcium. *J. Phys. B* **40**, 4023 (2007).
3. O. Zatsarinny, K. Bartschat, S. Gedeon, V. Gedeon, V. Lazur, E. Nagy. Cross sections for electron scattering from magnesium. *Phys. Rev. A* **79**, 052709 (2009).
4. E.A. Nady. Cross-sections of electron scattering by Sr atom. *Nauk. Visn. Uzhgorod. Nats. Univ. Ser. Fiz.* **25**, 148 (2009) (in Ukrainian).
5. V. Gedeon, S. Gedeon, V. Lazur, E. Nagy, O. Zatsarinny, K. Bartschat. Electron scattering from silicon. *Phys. Rev. A* **85**, 022711 (2012).
6. V. Gedeon, S. Gedeon, V. Lazur, E. Nagy, O. Zatsarinny, K. Bartschat. *B*-spline *R*-matrix-with-pseudostates calculations for electron-impact excitation and ionization of fluorine. *Phys. Rev. A* **89**, 052713 (2014).
7. V. Gedeon, S. Gedeon, V. Lazur, E. Nagy, O. Zatsarinny, K. Bartschat. *B*-spline *R*-matrix-with-pseudostates calculations for electron collisions with aluminum. *Phys. Rev. A* **92**, 052701 (2015).
8. L.O. Bandurina, S.V. Gedeon. Investigation of the concentration of electrons of plasma of glow-discharge above surface of aqueous solution of sulfate of aluminium. *Uzhhorod Univ. Sci. Herald. Ser. Phys.* **37**, 49 (2015).
9. O. Zatsarinny. BSR: *B*-spline atomic *R*-matrix codes. *Comput. Phys. Commun.* **174**, 273 (2006).
10. P.G. Burke, W.D. Robb. The *R*-matrix theory of atomic processes. *Adv. At. Mol. Opt. Phys.* **11**, 143 (1976).
11. V.P. Starodub, I.S. Aleksakhin, I.I. Garga, I.P. Zapesochnyi. *Opt. Spectrosc.* **35**, 1037 (1973).
12. I.S. Aleksakhin, I.I. Garga, I.P. Zapesochnyi, V.P. Starodub. *Opt. Spectrosc.* **37**, 20 (1974).
13. S.T. Chen, D. Leep, A. Gallagher. Excitation of the Sr and Sr^+ resonance lines by electron impact on Sr atoms. *Phys. Rev. A* **13**, 947 (1976).
14. S.M. Kazakov, N.I. Romanyuk, O.V. Khristoforov, O.B. Shpenik. Resonance effects observed under the interaction between slow-electrons and strontium atoms. *Opt. Spectrosc.* **59**, 22 (1985).

15. C. Froese-Fischer. The MCHF atomic-structure package. *Comput. Phys. Commun.* **64**, 369 (1991).
16. C. Froese-Fischer, T. Brage, O. Jonsson. *Computational Atomic Structure. An MCHF Approach* (CRC Press, 1997).
17. O. Zatsarinny, C. Froese-Fischer. Oscillator strengths for transitions to high-lying excited states of carbon. *J. Phys. B* **35**, 4669 (2002).
18. C.E. Moore. *Atomic Energy Levels as Derived from the Analysis of Optical Spectra. National Bureau of Standards Circular 467. Vol. III* (US Government Printing Office, 1958).
19. V. Gedeon, V. Lengyel, O. Zatsarinny, C.A. Kocher. Calculation of electron-impact excitation from metastable states of the Sr atom. *Phys. Rev. A* **56**, 3753 (1997).
20. I.I. Fabrikant. Collisions of slow electrons with atoms of alkaline elements. In *Atomic Processes*, edited by R.K. Peterkop (Zinatne, 1975), p. 80 (in Russian).
21. R. Szmytkowski, J.E. Sienkiewicz. Elastic scattering of electrons by strontium and barium atoms. *Phys. Rev. A* **50**, 4007 (1994).
22. J. Yuan. The resonance structures of electron interaction with Sr and Ba atoms: low-energy electron scattering and photodetachment of the negative ions. *J. Phys. B.* **36**, 2053 (2003).
23. M. Adibzadeh, C.E. Theodosiou. Elastic electron scattering from Ba and Sr. *Phys. Rev. A* **70**, 052704 (2004).
24. V.M. Burke, C.J. Noble. Farm – A flexible asymptotic R-matrix package. *Comput. Phys. Commun.* **85**, 471 (1995).
25. O.I. Zatsarinnyi, L.A. Bandurina, V.F. Gedeon. Resonances in electron-impact integral excitation cross sections of the magnesium atom. *Opt. Spectrosc.* **95**, 167 (2003).

Received 23.08.17.
Translated from Ukrainian by O.I. Voitenko

Є.А. Ноdь, В.Ф. Гедеон, С.В. Гедеон, В.Ю. Лазур

ЗБУДЖЕННЯ РЕЗОНАНСНОГО ПЕРЕХОДУ $5^1S - 5^1P^o$ АТОМА Sr ЕЛЕКТРОННИМ УДАРОМ

Р е з ю м е

Викладено основні аспекти нової версії методу R-матриці з B-сплайнами (BSR), що ґрунтується на використанні неортогональних орбіталей. Наближення BSR використане для розрахунків резонансної структури інтегральних перерізів переходу $5^1S \to 5^1P^o$ при розсіянні електронів на атомі стронцію в області енергій до 10 еВ. Для точного представлення хвильових функцій мішені використовувався багатоконфігураційний метод Хартрі–Фока з неортогональними орбіталями. Розклад у випадку сильного зв'язку включав 31 зв'язаний стан атома стронцію – від основного і аж до стану $5s5f\ ^1F^o$. Отримано добре узгодження розрахованих перерізів з наявними експериментальними даними і дана вичерпна теоретична інтерпретація останніх. Обговорено структуру резонансної особливості в перерізах розсіяння e-Sr в околі енергії 4 еВ.